The influence of shocks on star formation in the OMC1 Ridge

Astron. Astrophys. 248, L27–L30 (1991)

ASTRONOMY AND ASTROPHYSICS

Letter to the Editor

The influence of shocks on star formation in the OMC1 Ridge

J.S. Greaves and Glenn J. White

Department of Physics, Queen Mary and Westfield College (University of London), Mile End Road, LONDON E1 4NS, United Kingdom

Received June 6, accepted June 27, 1991

Abstract. Observations are presented of the OMC1 Ridge (a narrow band of molecular gas containing high-mass embedded sources), in the transitions CN N = 2 – 1, ^{13}CO J = 2 – 1 and ^{13}CS J = 5 – 4. Variations in velocities and line widths indicate that three distinct regions are present in the area mapped, and that at least one of these is rotating. The resulting shocks when these fragments collided will have compressed the gas to a density $n_{H_2} \sim 10^{7-8}$ cm^{-3}, sufficient to trigger collapse and to explain the presence of high-mass stars at the edges of the cloud fragments, rather than in their cores. These observational results support theoretical predictions of the importance of collisions in star formation.

Key words: interstellar medium: clouds: OMC1 – stars: formation of.

1. Introduction

The mechanisms which trigger star formation in molecular clouds are not yet fully understood. Cloud support is believed to be chiefly due to magnetic fields, since rotation speeds are generally low, and turbulence decays over short timescales (Shu et al., 1987). Magnetic field strengths B are unfortunately difficult to measure, and hence the critical mass ($M_{crit} \propto B^2$) which can be supported is hard to estimate in a particular cloud. For B $\sim$ 30 μG, a region $\sim$ 0.5 pc in size with mass $\geq$ 100 $M_\odot$ will collapse under gravity, and high-mass stars may form (Shu et al., 1987). Magnetic field strengths of 40 – 100 μG have been found over a 0.5 pc region of the HI envelope in front of OMC1 (Troland et al., 1989), hence an external force may be needed to overcome the strong cloud support.

Shocks have been suggested by several authors as a mechanism for triggering collapse (e.g. Elmegreen and Lada, 1977, Mundy et al., 1988; Rainey et al., 1987). Typically these models predict sequential star formation, with the expansion of ionisation fronts around young O and B type stars resulting in supersonic shocks in the surrounding molecular material. Fragmentation and compression of the shocked gas may produce dense cores which can no longer be magnetically supported, and collapse then occurs.

Send offprint requests to: J.S. Greaves

In the current paper, a different shock model is proposed to account for high-mass star formation in OMC1. A narrow ridge of dense gas has been observed in this cloud (Mundy et al., 1988), and two luminous IR sources, IRc2 and FIR4, both associated with molecular outflows (Wilson et al., 1986; Ziurys and Friberg, 1987), are embedded in the ridge gas. In this paper, the velocities in the region around these two young stars are examined, in order to estimate the importance of shocks.

2. Observations

Observations of the OMC1 Ridge were made during September 1989, using the 15 m James Clerk Maxwell Telescope (JCMT), situated on Mauna Kea, Hawaii. A strip of the cloud $\sim$ 7' in length was mapped in the transitions ^{13}CS J = 5 – 4, ^{13}CO J = 2 – 1 and hyperfine components of CN N = 2 – 1, as part of a search for chemical radicals (Greaves and White, 1991, in preparation). The line rest frequencies were taken to be 231,220.8 MHz, 220,398.7 MHz, and 226,632.8 – 226,892.9 MHz respectively. The beam width was 21" and pointing errors were typically 4", up to a maximum of 7". The (0,0) position was Right Ascension (1950) 05h 32m 47.0s, Declination (1950) –05° 24' 26", centred on the 'hot core' source, 2" south of IRc2. Points were observed on 3 parallel grids, angled 10° east of north, and these are shown in Figure 1, superimposed on an outline map of the ridge in HCN J = 3 – 2 (JCMT data obtained in October 1988).

The spectra are presented on scales of antenna temperature corrected for atmospheric and scattering losses (T_R^*) against local standard of rest velocity (v_{lsr}). Corrections to the velocity scale have been made using the frequency calibration curve measured by Redman (1990), which is believed to be stable to within $\ll$ 1 channel width. The s/n ratios of the lines are typically $\sim$ 20, hence the errors in the velocities are solely due to the finite spectrometer resolution, and are $\approx$ 0.45 km s^{-1}.

3. Results

The velocities of the line peaks, and the full widths at half maximum, are plotted against position offset in Figure 2. Three distinct regions are apparent in this diagram: to the north of IRc2 where $v_{lsr} \approx$ 10 km s^{-1}; between IRc2 and FIR4 where $v_{lsr} \approx$ 8.5 km s^{-1}; and south of FIR4 where

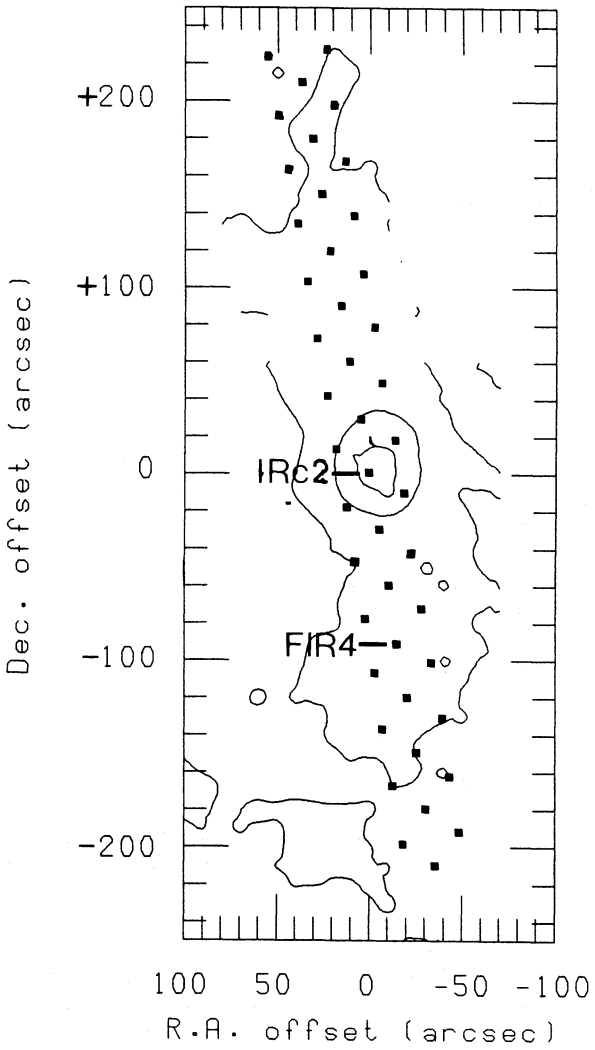

Fig. 1. Positions observed, superimposed on a HCN J = 3 – 2 outline map of the OMC1 ridge. Labels indicate the closest points to the embedded sources FIR4 and IRc2. The contours shown are 20, 120 and 220 K km s^{-1}, and the integration range was 10 km s^{-1} around the line peak at (0,0).

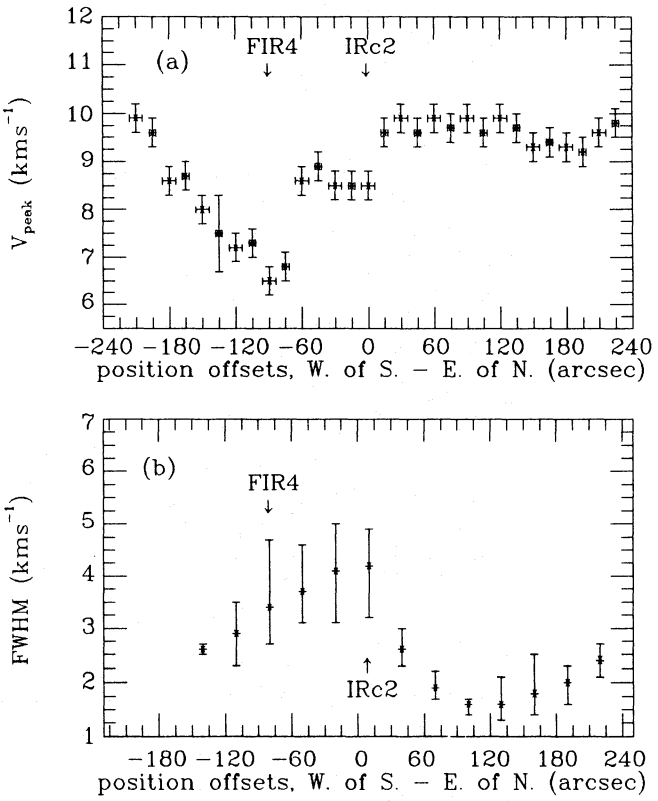

Fig. 2. Plots of (a) velocity of line peaks (v_{peak}) from ^{13}CO, and (b) full width at half maximum (FWHM) from CN, as a function of position in the ridge. The data points for the left and right grid axes have been averaged together; error bars reflect the spectrometer resolution and variations between grid points.

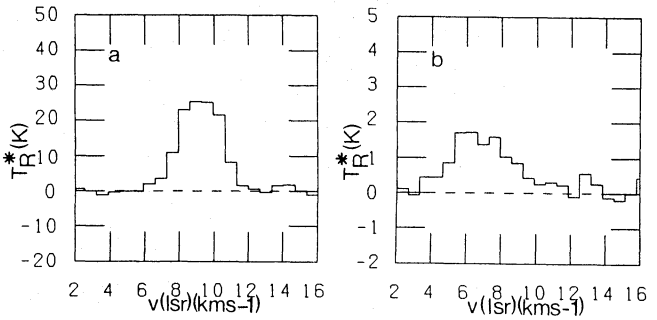

Fig. 3. Examples of (a) ^{13}CO J = 2 – 1 and (b) CN N = 2 – 1 spectra, centred on (δR.A., δDec. = +36", +207") from the (0,0) position.

there is a large velocity gradient ($\sim$ 12 km s^{-1} pc^{-1}). The full-width at the half-maxima are less for the north region, being only 1.8 $\pm$ 0.4 km s^{-1}, compared to 2.6 $\pm$ 0.5 km s^{-1} south of FIR4. (The values are measured from the strongest unblended CN hyperfine component, and the errors quoted are the 1σ variations.) This change of FWHM with position provides further evidence that at least two distinct regions are present.

South of FIR4, the large linear velocity gradient suggests that the gas is rotating. No shifts in velocity with position were found for the other two cloud regions, implying that rotation speeds are either small or in a direction close to the plane of the sky. Between 2' and 4' north of IRc2, there are indications of velocity shifts, but these are comparable to the errors. Evidence of rotation on 30" scales in this region has previously been reported by Harris et al. (1983), but this is not resolved in the current data.

There are some asymmetries in the line profiles, and also differences in v_{peak} between the ^{13}CO and CN data. These are mostly comparable to the velocity resolution, with the exception of the extreme north region, where a cloud with

$v_{lsr} \approx 7$ km s^{-1} was detected but the ^{13}CO emission at this velocity is blended with the main ridge emission at $v_{lsr} \approx 10$ km s^{-1} (Figure 3). These complexities in the line shapes make the results more difficult to analyse, but the existence of three distinct regions is clearly shown by the line peak velocities (Figure 2).

There has been considerable debate in the literature (e.g. Hasegawa et al., 1984; Vogel et al., 1985) as to whether IRc2 lies near the centre of a single rotating cloud, or between two clouds with velocities ≈ 8 and 10 km s^{-1}. The present data, covering a large section (1 pc) of the ridge with high spatial resolution, shows that there is an abrupt change of velocity at the IRc2 position, and another at FIR4, suggesting that *three* kinematically distinct cloud fragments are present. *The luminous high-mass sources IRc2 and FIR4 are located not in the centres of these regions, but at their intersections.* A model is therefore required to explain why star formation occurs at the fragment *edges*, rather than in the cores.

4. Star formation model

The observations do not have sufficient spatial coverage to provide a complete picture of the velocity structure in the three regions. The data can, however, be used to estimate the effects of shocks at the positions where there is an abrupt change of velocity.

The following scenario is proposed to explain the locations of high-mass star formation in OMC1. The cloud is observed to contain fragments with rotational and central velocities of different magnitudes and directions. When two such regions collide, the velocity discontinuity will result in a shock, which will compress the gas in the contact area. Where the density enhancement is sufficiently large, collapse can occur, leading to star formation not in the cores of the fragments, but at their edges, as observed. This qualitative model is supported by detailed hydrodynamical calculations of colliding gas flows (Hunter et al., 1986). Instabilities in a compressed collision zone were shown to accrete matter and subsequently collapse to form stars.

For the specific case of OMC1, a simple estimate has been made of the increase in the gas density in the collision zone. For an isothermal shocked region, $\rho_2/\rho_1 = v_{shock}^2/c_1^2$ (Schloerb and Loren, 1982), where ρ_2 and ρ_1 are the post- and pre-shock densities, and c_1 is the pre-shock sound speed in the gas, given by $c_1 = \sqrt{(\gamma k T_{kin}/m_{H_2})}$. In OMC1, $T_{kin} \sim 20 - 40$ K (from NH_3 observations by Batrla et al. (1983), and consistent with the peak antenna temperatures of ^{13}CO J = 2 – 1), and $\gamma = 7/5$ for diatomic hydrogen, resulting in a value for $c_1 \sim 0.3 - 0.5$ km s^{-1}. The shock speeds are the difference in velocity at the clump edges, and are 1.5 – 5 km s^{-1} (uncorrected for projection effects), from the current data and the higher spatial resolution observations of Vogel et al. (1985). Resulting compression factors are therefore $\sim 10 - 300$, but these values are likely to be underestimates, since ρ_2/ρ_1 values as high as 500 – 700 have been predicted for $v_{shock} = 5$ km s^{-1} (Hunter et al., 1986).

Large-scale velocity gradient (LVG) modelling of the ^{13}CS J = 5 – 4 data, together with CS J = 2 – 1 antenna temperatures from the maps of Mundy et al. (1988), has shown that $n_{H_2} \sim 10^6$ cm^{-3} in the densest parts of the southern ridge gas. Compression factors $\sim 10 - 300$ will therefore have resulted in an increase of density to $n_{H_2} \sim 10^{7-8}$ cm^{-3}, comparable to or larger than the observational threshold for collapse (densities higher than $\sim 10^7$ cm^{-3} are not observed in molecular clouds, Evans et al., 1987). The post-shock density in the collision zone is therefore consistent with the conditions in which stars are believed to form.

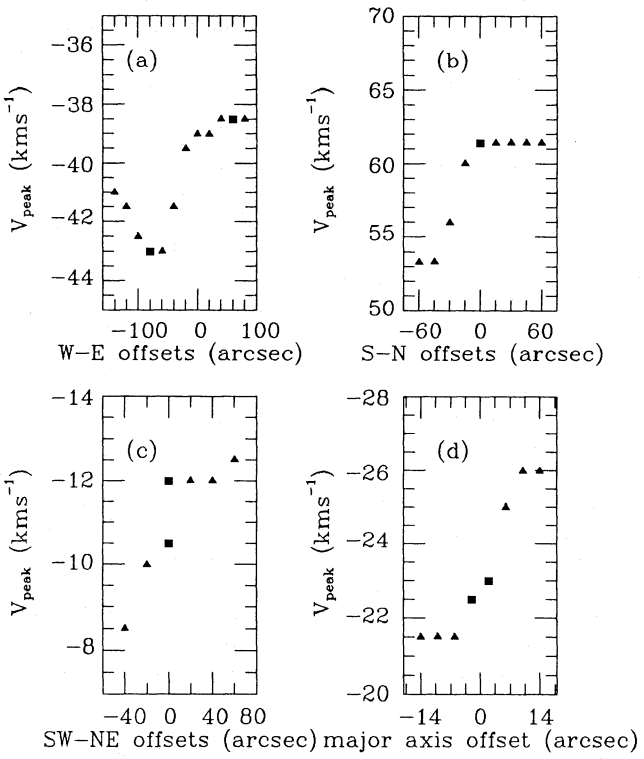

Fig. 4. Examples of velocity profiles in star formation regions. (a) W3, Hayashi et al., 1989 (b) Sgr B2, Goldsmith et al., 1987 (c) Ceph A, Torelles et al., 1986 (d) W58, Vogel and Welch, 1983. The square symbols mark the position(s) nearest to embedded sources.

It should be noted that even if the collision zone is considerably smaller than the diameters of the cloud fragments, the amount of material involved is sufficient to form a high-mass star. In OMC1, for a zone width of 30", for example, which is $\leq 1/3$ of the fragment widths, and column densities $N_{H_2} \sim 3 \times 10^{23}$ cm^{-2} (Blake et al., 1987), the mass of shocked gas is $\sim 25\ M_\odot$. Also, for a fragment diameter of ~ 0.2 pc and a shock speed of $\sim 1 - 5$ km s^{-1}, the free-fall time and the interval for the shock to cross the fragment are comparable (a few times 10^4 years). This supports the above model, since the collision zone will start to collapse first, before the shock has reached (and hence compressed) regions further into the fragment.

5. Discussion

Observations of other high-mass star-formation regions indicate that velocity shifts may be important in clouds apart from OMC1. The observed velocity profiles in W3, Cepheus A, W58 and Sagittarius B2 are plotted in Figure 4. Embedded high-

mass objects are again found at the positions of abrupt changes in velocity or velocity gradient. Discontinuities in these plots are generally not resolved, because of the greater distances of these sources, but it is significant that the locations of the sources are in all these cases at the fragment edges rather than the centres.

These results suggest that cloud collisions may be an important trigger of star formation. The small-scale mapping data therefore support the results of Scoville et al. (1986), who analysed the formation efficiency for O and B stars in a sample of 94 GMC's. They found least efficient high-mass star formation in the larger clouds, which have small surface-to-volume ratios. This suggested cloud-cloud collisions might trigger collapse, with lower efficiency in large clouds because only a small fraction of the gas is near the surface area involved in the impact.

It is unlikely that collisions are the only mechanism leading to high-mass star-formation, since shocks from HII region expansion are known to be important in clouds such as M17(SW), and there are also examples of clouds where stars have formed near clump centres (e.g Heyer et al., 1986). Magnetic field configurations in the fragments are presumably also important for the details of the collisional process, but there is insufficient data to include such effects. Comparative studies of all support mechanisms and triggers of collapse are therefore needed, to fully understand present rates of high-mass star formation in the Galaxy.

Acknowledgements. We wish to thank Dr. Nick Parker for assisting with the observations, and Dr. Russell Redman for advice on the velocity calibration. We are also grateful to the staff at the JCMT for their help at the telescope, and the U.K. Science and Engineering Research Council for travel funding, the support of millimetre and sub-millimetre astronomy at QMW, and a studentship for JSG. The JCMT is operated by the Royal Observatory, Edinburgh, on behalf of the SERC, the Netherlands Organisation for Pure Research, and the National Research Council of Canada.

References

Batrla, W., Wilson, T.L., Bastien, P., Ruf, K., 1983, A & A 128, 279

Blake, G.A., Sutton, E.C., Masson, C.R., Phillips, T.G., 1987, ApJ 315, 621

Elmegreen, B.G., Lada, C.J., 1977, ApJ 214, 725

Evans, N.J. II, Mundy, L.G., Davis, J.H., Vanden Bout, P., 1987, ApJ 312, 344

Goldsmith, P.F., Snell, R.L., Hasegawa, T., Ukita, N., 1987, ApJ 314, 525

Greaves, J.S., White, G.J., 1991 (in prep.)

Harris, A., Townes, C.H., Matsakis, D.N., Palmer, P., 1983, ApJ 265, L63

Hasegawa, T., Kaifu, N., Inatani, J., Morimoto, M., Chikada, Y., Hirabayashi, H., Iwashita, H., Morita, M., Tojo, A., Akabane, K., 1984, ApJ 283, 117

Hayashi, M., Kobayashi, H., Hasegawa, T., 1989, ApJ 340, 298

Heyer, M.H., Snell, R.L., Goldsmith, P.F., Strom, S.E., Strom, K.M., 1986, ApJ 308, 134

Hunter, J.H., Sandford, M.T., Whitaker, R.W., Klein, R.I., 1986, ApJ 305, 309

Mundy, L.G., Cornwell, T.J., Masson, C.R., Scoville, N.Z., Bååth, L.B., Johansson, L.E.B., 1988, ApJ 325, 382

Rainey, R., White, G.J., Gatley, I., Hayashi, S.S., Kaifu, N., Griffin, M.J., Monteiro, T.S., Cronin, N.J., Scivetti, A., 1987, A & A 171, 252

Redman, R.O., 1990, The AOS-C User's Manual, Volume IV

Schloerb, F.P., Loren, R.B., 1982, in Symposium on the Orion Nebula to honor Henry Draper, Ann. N. Y. Acad. Sci.

Scoville, N.Z., Sanders, D.B., Clemens, D.P., 1986, ApJ 310, L77

Shu, F.H., Adams, F.C., Lizano, S., 1987, Ann. Rev. Astr. Astrophys. 25, 23

Torelles, J.M., Ho, P.T.P., Rodríguez, L.F., Cantó, J., 1986, ApJ 305, 721

Troland, T.H., Heiles, C., Goss, W.M., 1989, ApJ 337, 342

Vogel, S.N., Bieging, J.H., Plambeck, R.L., Welch, W.J. and Wright, M.C.H., 1985, ApJ 296, 600

Vogel, S.N., Welch, W.J., 1983, ApJ 269, 568

Wilson, T.L, Serabyn, E., Henkel, C., Walmsley, C.M., 1986, A & A 158, L1

Ziurys, L.M., Friberg, P., 1987, ApJ 314, L49

This article was processed by the author using Springer-Verlag TEX AA macro package 1989.